Intramolecular interaction in LGN, an adaptor protein that regulates mitotic spindle orientation

Received for publication, October 11, 2019, and in revised form, November 7, 2019 Published, Papers in Press, November 15, 2019, DOI 10.1074/jbc.RA119.011457

Hiroki Takayanagi, Junya Hayase, Sachiko Kamakura, Kei Miyano, Kanako Chishiki, Satoru Yuzawa, and Hideki Sumimoto[1]

From the Department of Biochemistry, Kyushu University Graduate School of Medical Sciences, Fukuoka 812-8582, Japan

Edited by Patrick Sung

Proper mitotic spindle orientation requires that astral microtubules are connected to the cell cortex by the microtubule-binding protein NuMA, which is recruited from the cytoplasm. Cortical recruitment of NuMA is at least partially mediated via direct binding to the adaptor protein LGN. LGN normally adopts a closed conformation via an intramolecular interaction between its N-terminal NuMA-binding domain and its C-terminal region that contains four GoLoco (GL) motifs, each capable of binding to the membrane-anchored $G\alpha_i$ subunit of heterotrimeric G protein. Here we show that the intramolecular association with the N-terminal domain in LGN involves GL3, GL4, and a region between GL2 and GL3, whereas GL1 and GL2 do not play a major role. This conformation renders GL1 but not the other GL motifs in a state easily accessible to $G\alpha_i$. To interact with full-length LGN in a closed state, NuMA requires the presence of $G\alpha_i$; both NuMA and $G\alpha_i$ are essential for cortical recruitment of LGN in mitotic cells. In contrast, mInsc, a protein that competes with NuMA for binding to LGN and regulates mitotic spindle orientation in asymmetric cell division, efficiently binds to full-length LGN without $G\alpha_i$ and induces its conformational change, enhancing its association with $G\alpha_i$. In nonpolarized symmetrically dividing HeLa cells, disruption of the LGN–NuMA interaction by ectopic expression of mInsc results in a loss of cortical localization of NuMA during metaphase and anaphase and promotes mitotic spindle misorientation and a delayed anaphase progression. These findings highlight a specific role for LGN-mediated cell cortex recruitment of NuMA.

Cell division is fundamental for increasing cell number and altering cell types; cells divide symmetrically to expand the number of identical cells, whereas asymmetric cell divisions regulate differentiation by generating two different daughter cells (1–4). During mitosis, microtubules reorganize into bipolar spindles that attach the chromosomes to the centrosomes (*i.e.* the spindle poles) and into astral microtubules that emanate from the spindle poles and attach to the actin-rich cell cortex. The cortical capture of astral microtubules is followed by the localization of the minus-end-directed motor protein complex dynein at the cell cortex. The movement of cortically anchored dynein on the astral microtubules toward the spindle poles is thought to generate pulling forces for correct positioning of the spindle poles and proper spindle orientation (5–7). Cortical recruitment of the motor complex involves the dynein-binding protein NuMA, a component of an evolutionarily-conserved ternary complex containing the adaptor protein LGN and the $G\alpha_i$ subunit of heterotrimeric G proteins (5–7).

In symmetric cell division of adherent mammalian cells, including nonpolarized HeLa cells, LGN forms a complex with NuMA and GDP-bound $G\alpha_i$ during metaphase, the latter of which is directly anchored in the plasma membrane (8–13). NuMA is thus targeted to the lateral cortex via ternary complex formation to recruit its partner dynein for planar spindle orientation (9–13). mInsc, another LGN-binding protein (14, 15), drives asymmetric cell division in mammalian cells with apico-basal polarity, such as epidermal and neuronal progenitor cells, via influencing spindle orientation from planar toward more apico-basal orientation (14, 16–19). This effect is likely mediated via apical recruitment of LGN by the adaptor mInsc, which is able to simultaneously bind to Par3 (15), a cell polarity protein that localizes to the apical membrane in these cells (14, 16–19).

Human LGN directly interacts with NuMA and mInsc via the N-terminal domain, comprising eight copies of tetratricopeptide repeat (TPR)[2] motif (20–25), whereas the C-terminal region of LGN contains four GoLoco (GL) motifs, each capable of binding to GDP-bound $G\alpha_i$ (26, 27) (see Fig. 1*A*). Since the NuMA-binding site overlaps with the mInsc-interacting region, the two proteins bind to LGN in a mutually exclusive manner (20, 21). The four GL motifs (GL1–GL4) in LGN are intrinsically independent $G\alpha_i$-binding sites with a similar affinity (26, 27). During interphase, LGN adopts a closed conformation via an intramolecular interaction of the N-terminal TPR domain with a C-terminal GL-motif-containing region (8, 28). Full-length LGN, in the closed structure, appears to marginally interact with NuMA and $G\alpha_i$, compared with the isolated TPR domain and C-terminal region, respectively (8). Although mInsc interacts with the N-terminal fragment of LGN with a

This work was supported in part by Ministry of Education, Culture, Sports, Science and Technology Grant-in-Aid for Scientific Research on Innovative Areas "Oxygen Biology: a new criterion for integrated understanding of life" JP26111009 (to H. S.); and Japan Society for the Promotion of Science KAKENHI Grant JP18K06934 (to S. K.). The authors declare that they have no conflicts of interest with the contents of this article.

[1] To whom correspondence should be addressed: Dept. of Biochemistry, Kyushu University Graduate School of Medical Sciences, Fukuoka 812-8582, Japan. E-mail: hsumi@med.kyushu-u.ac.jp.

[2] The abbreviations used are: TPR, tetratricopeptide repeat; CBB, Coomassie Brilliant Blue; DMEM, Dulbecco's modified Eagle's medium; FCS, fetal calf serum; GL, GoLoco; GST, glutathione *S*-transferase; MBP, maltose-binding protein; MDCK, Madin–Darby canine kidney.

higher affinity than that of NuMA (20, 21), it has been obscure whether the same is true on the interaction with full-length LGN.

The *Drosophila* LGN-related protein Pins also forms a closed state via a similar intramolecular TPR–GL interaction (29), although it lacks a GL motif, corresponding to the second GL motif (GL2) in mammalian LGN, and thus contains only three GL motifs (30). The first GL motif in Pins does not seem to be coupled to the intramolecular interaction, in contrast to the other two motifs; full-length Pins is capable of binding to $G\alpha_i$ via the first GL motif (29). On the other hand, in human LGN, all the four GL motifs are thought to be required for the intramolecular interaction (8, 28), suggesting that the activity of LGN and Pins may be differentially regulated. The precise regulation of LGN, however, has not been well-understood.

In the present study, we show that the intramolecular interaction with the TPR domain in LGN involves GL3, GL4, and a region between GL2 and GL3, whereas GL1 and GL2 do not play major roles. This conformation renders GL1 but not other GL motifs in a state easily accessible to $G\alpha_i$. The TPR-binding protein mInsc efficiently interacts with full-length LGN and induces its conformational change to enhance the association with $G\alpha_i$ via GL motifs other than GL1. In contrast, NuMA, another target for LGN-TPR, requires the presence of $G\alpha_i$ for its binding to full-length LGN; both NuMA and $G\alpha_i$ are essential for cortical recruitment of LGN in mitotic cells. Disruption of the LGN–NuMA interaction by mInsc results in a loss of cortical localization of NuMA during metaphase and anaphase, which leads to mitotic spindle misorientation and a delayed anaphase progression.

Results

A region required for intramolecular interaction with the N-terminal TPR domain of LGN

In LGN, the N-terminal TPR domain directly associates with the C-terminal region, which contains four copies of the GL motif, a conserved sequence of 19 amino acids (30) (Fig. 1*A*). To precisely map a region required for the intramolecular interaction with the N-terminal domain (LGN-N, amino acids 13–414), we prepared a series of C-terminal fragments as MBP (maltose-binding protein)-fused protein and performed an MBP pulldown binding assay. As shown in Fig. 1*B*, a C-terminal fragment that lacks GL1 (amino acids 535–645) or both GL1 and GL2 (560–645) associated with LGN-N as strongly as the C-terminal region of LGN (LGN-C) that contains the four GL motifs (480–645). Thus, GL1 and GL2 do not seem to play a major role in the intramolecular interaction. On the other hand, further deletion of a region between GL2 and GL3 (560–580) resulted in an incomplete but severe loss of the interaction (Fig. 1*B*), indicating the significance of the region linking GL2 and GL3. The finding also suggests a significant role of GL3, GL4, or both in the intramolecular interaction in LGN. Indeed both regions are likely required, because a fragment lacking GL3 (619–645) or GL4 (560–611 or 581–611) was incapable of interacting with LGN-N (Fig. 1*C*). Taken together, GL3, GL4, and the linker region between GL2 and GL3 appear to participate in the intramolecular interaction with the N-terminal TPR domain.

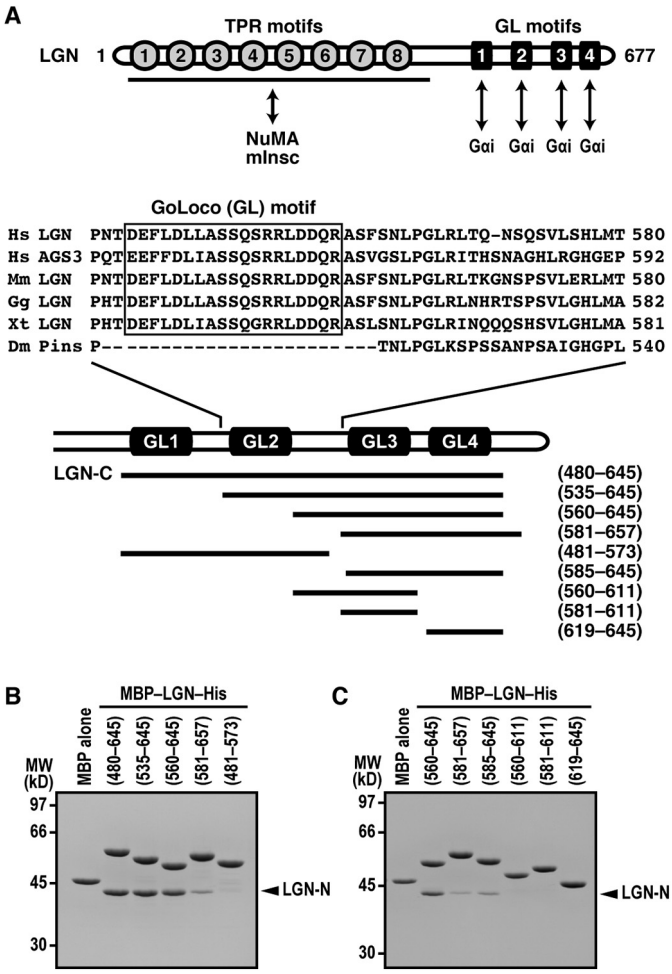

Figure 1. A region required for intramolecular interaction with the N-terminal TPR domain in LGN. *A*, schematic representation of the domain organization of human LGN and its truncated proteins used in the present study. The N-terminal domain of LGN comprises eight TPR motifs, whereas the C-terminal region contains four GL motifs. GL2 and its C-terminally flanking region of LGN-related proteins from various species are aligned: *Homo sapiens* (*Hs*), *Mus musculus* (*Mm*), *Gallus gallus* (*Gg*), *Xenopus tropicalis* (*Xt*), and *Drosophila melanogaster* (*Dm*). The core conserved sequences of the GL motif are *boxed*. *B* and *C*, MBP-fused LGN with the indicated truncation or MBP alone was incubated with LGN-N and pulled down with amylose resin. The precipitated proteins were subjected to SDS-PAGE, followed by staining with CBB. The positions for marker proteins are indicated in kilodaltons. *MW*, molecular weight.

GL1 in full-length LGN is easily accessible to $G\alpha_i$

The present findings that GL3 and GL4 but not GL1 or GL2 play a major role in the intramolecular interaction of LGN (Fig. 1) raised the possibility that GDP-bound $G\alpha_i$ may access GL1 and/or GL2 more easily than GL3 and GL4 in full-length LGN (LGN-F, amino acids 1–677). To test this, we introduced mutations that led to a loss of binding to $G\alpha_i$ in both GL1 and GL2 or in both GL3 and GL4. It is well known that the $G\alpha_i$-binding activity of the GL motif is almost completely lost by substitution of phenylalanine for arginine, which is the rearmost residue in the conserved 19 amino acid sequence of GL motifs (29–31); the invariant arginine residue corresponds to Arg-501 of GL1, Arg-556 of GL2, Arg-606 of GL3, and Arg-640 of GL4 in human

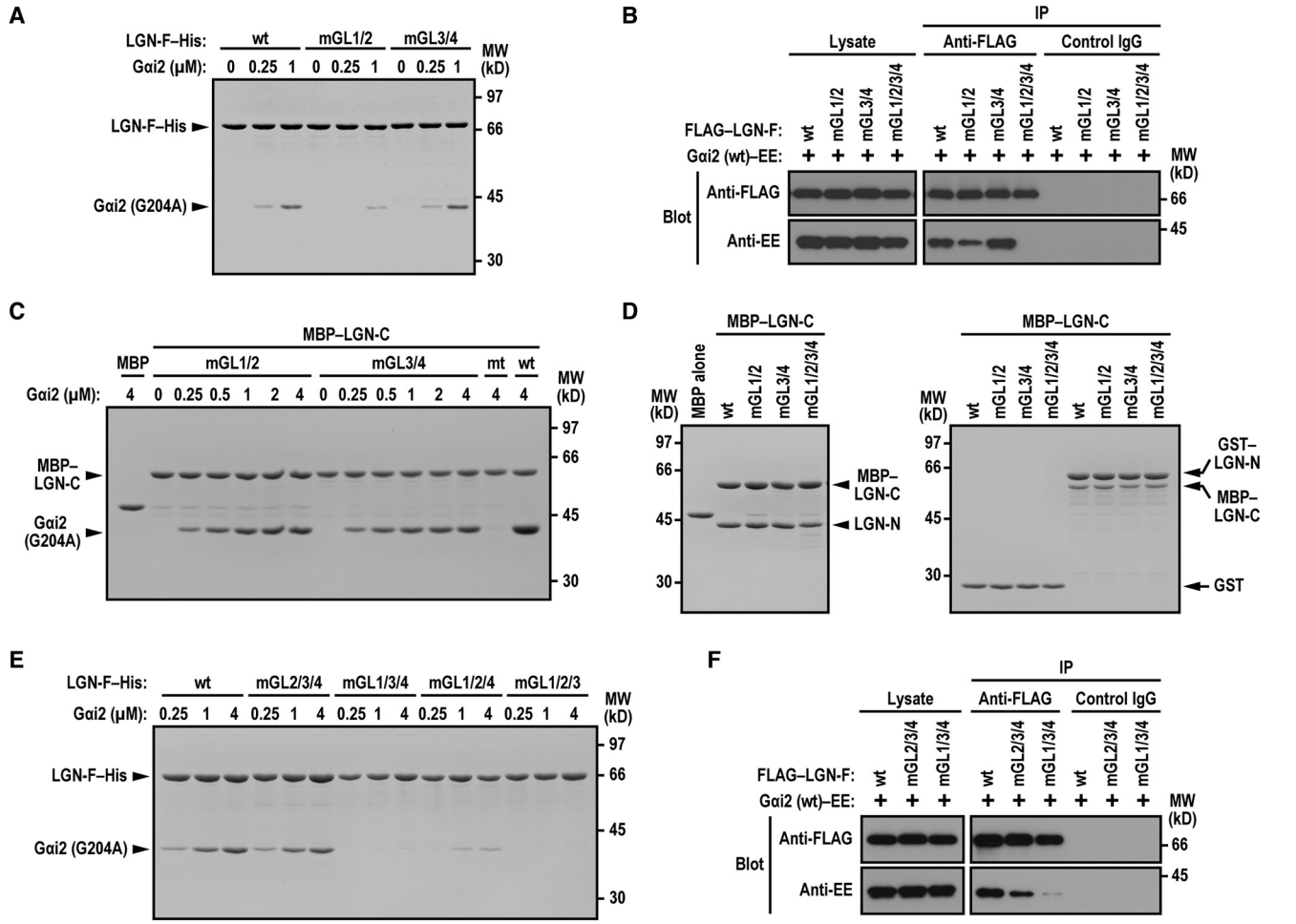

Figure 2. GL1 in full-length LGN is easily accessible to Gα_i. *A*, *C*, and *E*, Gα_{i2} (G204A) at the indicated concentrations was incubated with 0.5 μM LGN-F-(1–677)–His (*A* and *E*) or with 0.5 μM MBP-LGN-C-(480–645)–His or MBP alone (*C*). Proteins were pulled down with COSMOGEL His-Accept (*A* and *E*) or amylose resin (*C*) and subjected to SDS-PAGE, followed by staining with CBB. *B* and *F*, FLAG–LGN-F (wt or the indicated mutant protein) and Gα_{i2} (wt)–EE were expressed in HEK293 cells, and proteins in the cell lysate were immunoprecipitated (*IP*) with the anti-FLAG antibody, followed by immunoblot analysis with the indicated antibodies (*Blot*). *D*, MBP–LGN-C–His or MBP alone was incubated with LGN-N (*left panel*) or with GST–LGN-N or GST alone (*right panel*). Proteins were pulled down with amylose resin (*left panel*) or glutathione-Sepharose-4B beads (*right panel*) and subjected to SDS-PAGE, followed by staining with CBB. Positions for marker proteins are indicated in kilodaltons. *MW*, molecular weight. *wt*, wild-type: *mGL1/2*, *mGL3/4*, *mGL2/3/4*, *mGL1/3/4*, *mGL1/2/4*, *mGL1/2/3*, and *mGL1/2/3/4* or *mt*, the R501F/R556F, R606F/R640F, R556F/R606F/R640F, R501F/R606F/R640F, R501F/R556F/R640F, R501F/R556F/R606F, and R501F/R556F/R606F/R640F substitutions, respectively.

LGN. Using purified full-length LGN proteins carrying mutated GL1/GL2 (LGN-F-mGL1/2 with the R501F/R556F substitution) and with mutated GL3/GL4 (LGN-F-mGL3/4 with the R606F/R640F substitution), we investigated their ability to bind to Gα_{i2}–GDP. Although LGN-F-mGL1/2 failed to effectively bind to the GDP-bound form of Gα_{i2} (G204A), LGN-F-mGL3/4 interacted with Gα_{i2} (G204A) to a similar extent to WT LGN-F (Fig. 2*A*). Similarly, when WT and mutant LGN-F proteins were expressed as FLAG-tagged protein in HEK293 cells, EE-tagged Gα_{i2} was co-precipitated with LGN-F-mGL1/2 but to a lesser extent than that with LGN-F-mGL3/4 and with the WT protein (Fig. 2*B*). These findings suggest that GL1 and/or GL2 in full-length LGN is more easily accessible to Gα_{i2}.

The difference in the accessibility is not likely due to that in their Gα_{i2}-binding activity. This is because, in contrast to full-length proteins, C-terminal fragments (amino acids 480–645) with the mutations (LGN-C-mGL1/2 and LGN-C-mGL3/4) interacted with Gα_{i2} (G204A) to the same extent (Fig. 2*C*), which is consistent with previous observations that four GL motifs of LGN each bind to Gα_i with a similar affinity (26, 27). In addition, LGN-C-mGL1/2 and LGN-C-mGL3/4 associated with LGN-N as strongly as the WT protein (Fig. 2*D*), confirming that both R501F/R556F and R606F/R640F substitutions do not affect the intramolecular interaction in LGN.

We next asked which is responsible for the easy Gα_i accessibility, GL1 or GL2. As shown by an *in vitro* binding assay using purified protein, LGN-F-mGL2/3/4, in which GL1 is solely intact among the four motifs, associated with Gα_{i2} as effectively as the WT protein (Fig. 2*E*). In contrast, GL2, as well as GL3 and GL4, in full-length LGN was less effective in binding to Gα_{i2} (Fig. 2*E*). Also in HEK293 cells, LGN-F-mGL2/3/4 (with active GL1) bound more efficiently to Gα_{i2} than did LGN-F-mGL1/3/4 (with active GL2) (Fig. 2*F*). Thus, GL1 in full-length LGN is easily accessible to Gα_i, indicating that GL1 is in a state capable of interacting with Gα_i even in the presence of the intramolecular interaction.

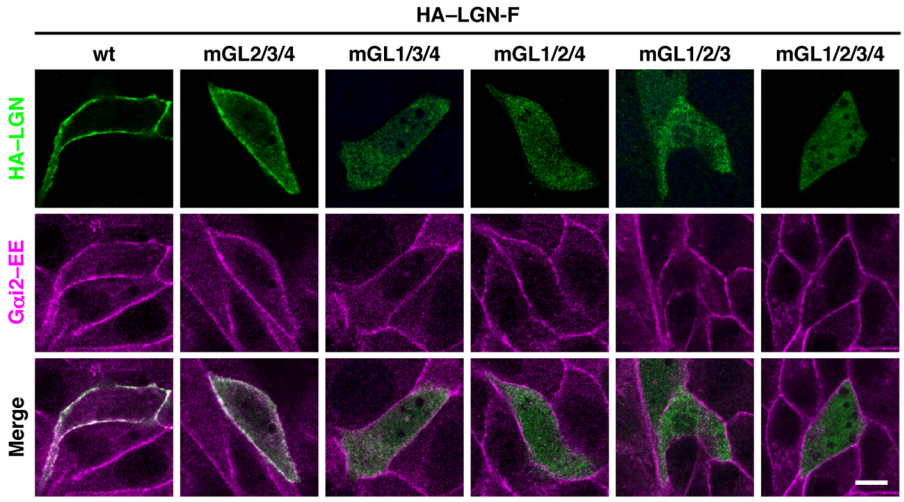

Figure 3. GL1 but not other GLs in full-length LGN is accessible to $G\alpha_{i2}$ expressed on the plasma membrane in MDCK cells. MDCK cells stably expressing EE-tagged $G\alpha_{i2}$ (wt) were transfected with pFE-BOS encoding an HA-tagged full-length LGN as follows: WT LGN (wt); a mutant protein with active GL1 (mGL2/3/4), GL2 (mGL1/3/4), GL3 (mGL1/2/4), or GL4 (mGL1/2/3); or a mutant protein with the four GLs inactivated (mGL1/2/3/4). The cells were fixed and stained with the anti-HA (*green*) and anti-EE (*magenta*) antibodies. *Scale bar*, 10 μm.

GL1 of LGN is accessible to $G\alpha_{i2}$ expressed on the plasma membrane in MDCK cells

As shown here, among the four GL motifs in LGN, GL1 is in a state easily accessible to $G\alpha_i$ (Fig. 2). To further investigate the *in vivo* structure of LGN, we expressed mutant full-length LGN proteins with a single intact GL motif and the other three motifs inactivated. In MDCK cells overexpressing $G\alpha_{i2}$, full-length LGN (wt) localized to the cell cortex (Fig. 3). On the other hand, LGN (wt) was distributed throughout the cytoplasm of parent MDCK cells (data not shown). These findings indicate that LGN by itself is capable of localizing to the cell cortex in the presence of enough amounts of $G\alpha_i$ on the plasma membrane. LGN-F-mGL2/3/4 (with active GL1) also localized to the cell cortex but to a lesser extent (Fig. 3), suggesting that GL1 is easily accessible to $G\alpha_{i2}$ on the plasma membrane and that a single GL motif has an ability to localize LGN to the cell cortex. On the other hand, cortical localization was lost by inactivation of GL1 and any two of the other three GL motifs (Fig. 3). Thus, GL2, GL3, and GL4 in full-length LGN appear to be inaccessible to $G\alpha_{i2}$. The crucial role of GL1 in cortical recruitment of LGN is consistent with the present binding assays using full-length LGN both *in vivo* and *in vitro* (Fig. 2).

mInsc but not NuMA binds to LGN even in the absence of $G\alpha_i$

In vitro, mInsc directly binds to the N-terminal TPR domain of LGN with a higher affinity than that of NuMA (20, 21). Here we compared the binding of full-length LGN (LGN-F) to NuMA with that to mInsc in HEK293 cells ectopically expressing $G\alpha_{i2}$ (G204A), because binding of LGN-F to NuMA is known to depend on the expression of $G\alpha_i$ (8). As shown in Fig. 4*A*, LGN-F interacted with full-length mInsc (mInsc-F) much more strongly than with full-length NuMA (NuMA-F), suggesting that mInsc may bind to LGN-F independently of the presence of $G\alpha_i$. We next tested this possibility both by an *in vitro* binding assay using purified LGN-F and by a co-precipitation assay in cells expressing full-length proteins. Purified LGN-F interacted with the LGN-interacting region of NuMA (amino acids 1885–1912) solely in the presence of $G\alpha_i$ (Fig. 4*B*). In contrast, even without $G\alpha_i$, LGN-F bound to the LGN-binding domain of mInsc (amino acids 23–69) (Fig. 4*B*). When expressed in HEK293 cells, LGN-F interacted with NuMA-F in a manner completely dependent on co-expression with $G\alpha_{i2}$ (G204A) (Fig. 4*C*). In contrast, LGN-F bound to mInsc-F even in the absence of exogenous $G\alpha_{i2}$ (Fig. 4*D*). These findings indicate that full-length LGN is in a state accessible to mInsc at least to some extent, both *in vivo* and *in vitro*.

mInsc induces a conformational change of LGN to enhance its binding to $G\alpha_i$

Since NuMA is able to enhance LGN binding to $G\alpha_i$ (8), mInsc, a stronger partner of LGN (Fig. 4), is also expected to induce a conformational change in LGN. As shown in Fig. 5*A*, mInsc enhanced LGN binding to $G\alpha_i$ in a dose-dependent manner, which was more effective than that induced by NuMA. The mInsc-induced conformational change requires direct interaction with LGN, since the enhancement of LGN binding to $G\alpha_{i2}$ was impaired by the W31A/E42R substitution in mInsc (Fig. 5*B*), a mutation that leads to a defective interaction with LGN (20). In addition, mInsc blocked the association between the N- and C-terminal regions of LGN (Fig. 5*C*). Thus, mInsc induces a conformational change via disrupting the intramolecular interaction, which leads to enhancement of LGN binding to $G\alpha_i$.

The present finding that GL1 is ready to access $G\alpha_i$ even in a resting conformation suggests that the mInsc-induced conformational change promotes $G\alpha_i$ binding to GL motifs other than GL1. As expected, interaction with $G\alpha_i$ was efficiently enhanced in LGN-F-mGL1/2 (with intact GL3/4) but only slightly facilitated in LGN-F-mGL3/4 (with intact GL1/2) (Fig. 5*D*). Furthermore, mInsc did not affect GL1 binding to $G\alpha_i$ (see LGN-F-mGL2/3/4) but enhanced GL2 binding to $G\alpha_i$ (see LGN-F-mGL1/3/4) (Fig. 5*E*). These findings indicate that mInsc binding to LGN induces a conformational change, rendering GL motifs other than GL1 in a state accessible to $G\alpha_i$.

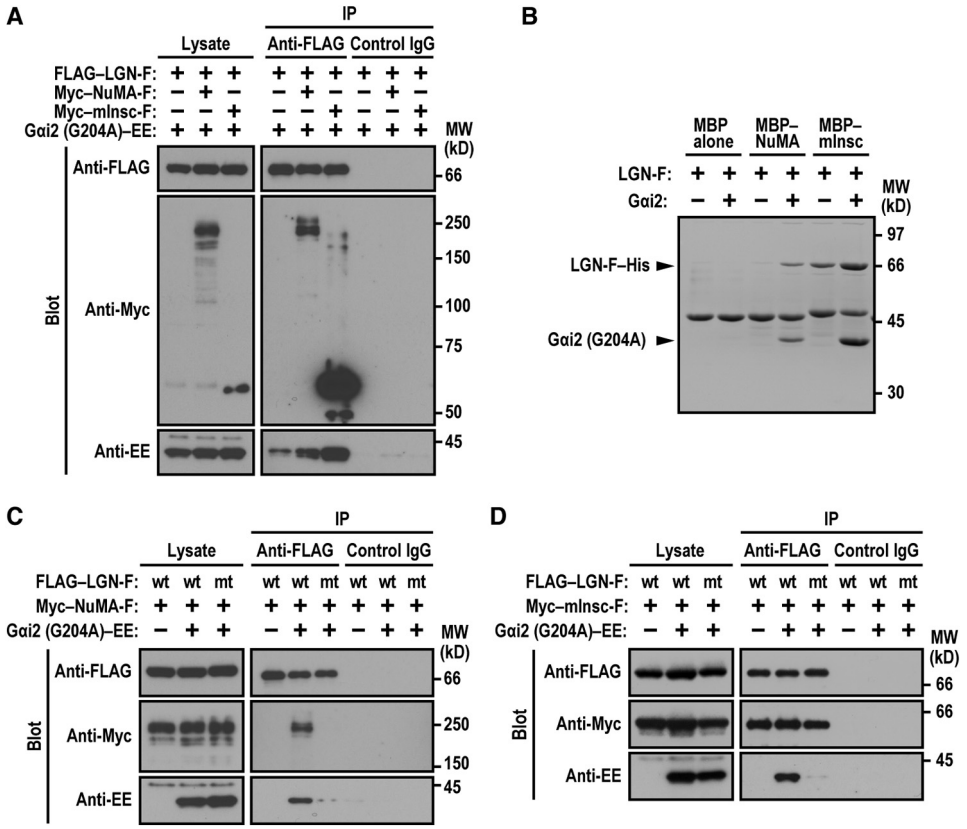

Figure 4. mInsc but not NuMA binds to LGN even in the absence of Gα_i. *A*, *C*, and *D*, FLAG–LGN-F was co-expressed with Myc–NuMA-F, Myc–mInsc-F, and/or Gα_{i2} (G204A)–EE in HEK293 cells, and proteins in the cell lysate were immunoprecipitated (*IP*) with the anti-FLAG antibody, followed by immunoblot analysis with the indicated antibodies (*Blot*). *B*, MBP–NuMA-(1885–1912), MBP–mInsc-(23–69), or MBP alone was incubated with purified LGN-F–His in the presence or absence of Gα_{i2} (G204A) and pulled down with amylose resin. The precipitated proteins were subjected to SDS-PAGE, followed by staining with CBB. Positions for marker proteins are indicated in kilodaltons. *MW*, molecular weight. *wt*, WT LGN-F; *mt*, a mutant LGN-F with the four GLs inactivated (mGL1/2/3/4).

Cortical recruitment of LGN during metaphase requires its simultaneous interaction with NuMA and Gα_i

In mitotic HeLa cells, LGN is enriched as two cortical crescents overlying each spindle pole during metaphase and anaphase (8–13). To clarify the role of NuMA as well as Gα_i in cortical association of LGN, we expressed full-length mutant LGN proteins, which led to defective binding to NuMA or Gα_i, in HeLa cells. Zhu *et al.* (21) have shown that alanine substitution of both Arg-221 and Arg-236 in LGN results in a loss of interaction with the LGN-binding region of NuMA. Consistent with this, a mutant LGN (R221A/R236A) failed to bind to full-length NuMA (Fig. 6*A*) but retained the ability to interact with mInsc (Fig. 6*B*). In contrast to cortical localization of WT LGN during metaphase, LGN-F (R221A/R236A) was distributed throughout the cytoplasm but not recruited to the cell cortex (Fig. 6*C*). Thus, interaction with NuMA appears to be required for localization of LGN to two cortical crescents facing the spindle poles. Cortical recruitment of LGN was also impaired by inactivation of all the four GL motifs (mGL1/2/3/4) (Fig. 6*C*), which leads to a complete loss of interaction with Gα_i (Figs. 2 and 4). These findings indicate that LGN is enriched in cortical crescents facing the spindle poles during metaphase via simultaneous interactions with NuMA and Gα_i.

Exogenous mInsc inhibits cortical localization of NuMA and correct spindle orientation

Because mInsc binds to LGN with a much higher affinity than that of NuMA and the NuMA-interacting site is mostly overlapped in the mInsc-binding region in LGN, mInsc effectively replaces NuMA in an *in vitro* biding assay using purified proteins (20, 21). Also in HeLa cells, mInsc is likely capable of dissociating the LGN–NuMA complex, since GFP-fused mInsc (wt) was enriched as two cortical crescents overlying each spindle pole during metaphase, and the expression resulted in a loss of cortical recruitment of NuMA without impairing its localization to the two spindle poles (Fig. 7*A*). In contrast, a mutant mInsc (W31A/E42R), defective in binding to LGN (20), localized throughout the cytoplasm and did not affect NuMA localization to the cortical crescents (Fig. 7*A*). These findings indicate that mInsc localizes to the cortex via the interaction with LGN and thereby dissociates NuMA from the LGN–NuMA complex.

In polarized mammalian cells such as epidermal and neuronal progenitor cells, apically expressed mInsc recruits LGN to the apical membrane and converts from planar into oblique/vertical orientation of mitotic spindles, leading to asymmetric cell division (14, 16–19). In these cases, it is thought that NuMA is recruited to the apical domain via binding to LGN (16–19),

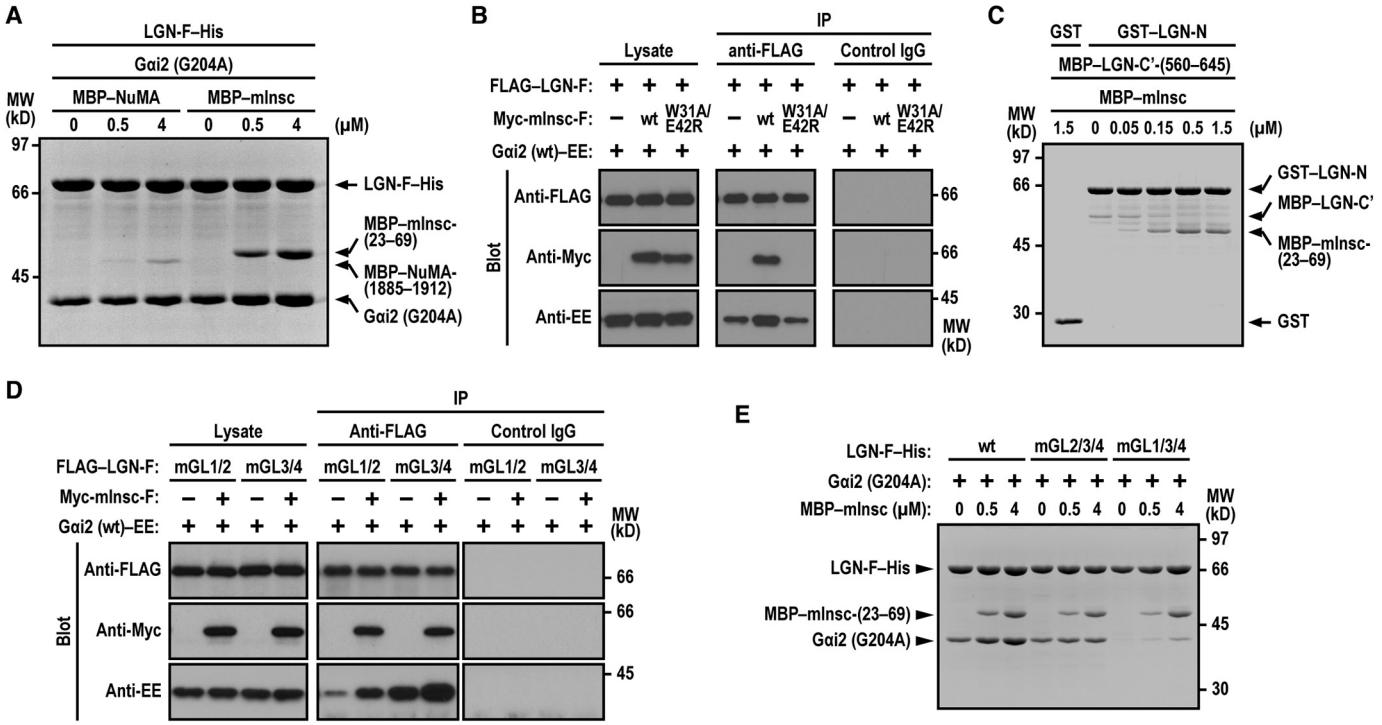

Figure 5. mInsc induces a conformational change of LGN to enhance its binding to $G\alpha_i$. *A* and *E*, LGN-F–His (0.5 μM) and $G\alpha_{i2}$ (G204A) (1 μM) were incubated with the indicated concentrations of MBP–NuMA-(1885–1912) (*A*) or MBP–mInsc-(23–69) (*A* and *E*) and pulled down with COSMOGEL His-Accept. The precipitated proteins were subjected to SDS-PAGE, followed by staining with CBB. *B* and *D*, FLAG–LGN-F (wt or the indicated mutant protein) and $G\alpha_{i2}$ (G204A)–EE were co-expressed with Myc–mInsc-F (wt) (*B* and *D*) or Myc–mInsc-F (W31A/E42R) (*B*) in HEK293 cells, and proteins in the cell lysate were immunoprecipitated (*IP*) with the anti-FLAG antibody, followed by immunoblot analysis with the indicated antibodies (*Blot*). *C*, GST–LGN-N (0.5 μM) or GST alone (0.5 μM) was incubated with MBP–LGN-C′-(560–645)–His (1.5 μM) and the indicated concentrations of MBP–mInsc-(23–69). Proteins pulled down with glutathione-Sepharose-4B beads were subjected to SDS-PAGE and stained with CBB. Positions for marker proteins are indicated in kilodaltons. *MW*, molecular weight. *wt*, WT; *mGL1/2*, *mGL3/4*, *mGL2/3/4*, and *mGL1/3/4*, the R501F/R556F, R606F/R640F, R556F/R606F/R640F, and R501F/R606F/R640F substitutions, respectively.

but the role of the LGN–NuMA interaction is questioned because mInsc and NuMA interact with LGN in a mutually exclusive manner. In nonpolarized mammalian adherent cells, such as HeLa cells, mitotic spindles are aligned parallel to the adhesion plane during symmetric cell division, which involves LGN and NuMA (8–13). To know the specific role of the LGN–NuMA interaction, we examined the effect of mInsc (wt) and mInsc (W31A/E42R) on planar spindle orientation in HeLa cells. The planar alignment of mitotic spindles was perturbed by expression of GFP–mInsc (wt) (Fig. 7, *B* and *C*). This effect appears to be mediated by LGN, since the perturbation was not induced by expression of GFP–mInsc (W31A/E42R), defective in binding to LGN (Fig. 7, *B* and *C*). Thus, mInsc-mediated blockade of the LGN–NuMA interaction results in spindle misorientation in metaphase HeLa cells. Taken together, the LGN–NuMA interaction is required for cortical localization of NuMA, which plays a role in planar spindle orientation in HeLa cells.

Exogenous mInsc blocks mitotic progression from metaphase to anaphase

Similar to the effect of mInsc on localization of endogenous NuMA during metaphase (Fig. 7*A*), the protein failed to fully localize to cortical crescents also during anaphase in HeLa cells expressing GFP–mInsc (wt) but not in those containing GFP–mInsc (W31A/E42R), impaired in binding to LGN (Fig. 8*A*). On the other hand, spindle pole accumulation of NuMA during anaphase was not affected by GFP–mInsc (wt) (Fig. 8*A*). Thus, mInsc-mediated blockade of the NuMA–LGN interaction likely inhibits cortical localization of NuMA in anaphase as well as in metaphase. These findings suggest that the NuMA–LGN interaction may play a role not only during metaphase but also at later mitotic stages. To test the possibility, we expressed mInsc (wt) or mInsc (W31A/E42R) in HeLa cells and analyzed mitotic cells by immunofluorescence detection (Fig. 8*B*). As shown in Fig. 8*C*, expression of GFP–mInsc (wt) marginally increased the number of mitotic cells, whereas GFP–mInsc (W31A/E42R) did not affect the mitotic index. Interestingly, solely in GFP–mInsc (wt)-expressing cells, the population of metaphase cells was elevated with a decrease in the sum of anaphase and telophase cells (Fig. 8*D*). We observed no difference between GFP-, GFP–mInsc (wt)-, and GFP–mInsc (W31A/E42R)-expressing cells in populations with defects in chromosome segregations such as misaligned chromosomes or lack of tension, suggesting that the mitotic checkpoint is not activated in GFP–mInsc (wt)-expressing cells (32). Thus, the LGN-mediated cortical localization of NuMA appears to be involved in mitotic progression from metaphase to anaphase.

Discussion

In the present study, we depict a closed structure of human LGN via analyses using purified proteins and by expressing mutant proteins in cells. LGN is known to adopt a closed conformation via the intramolecular interaction of the N-terminal

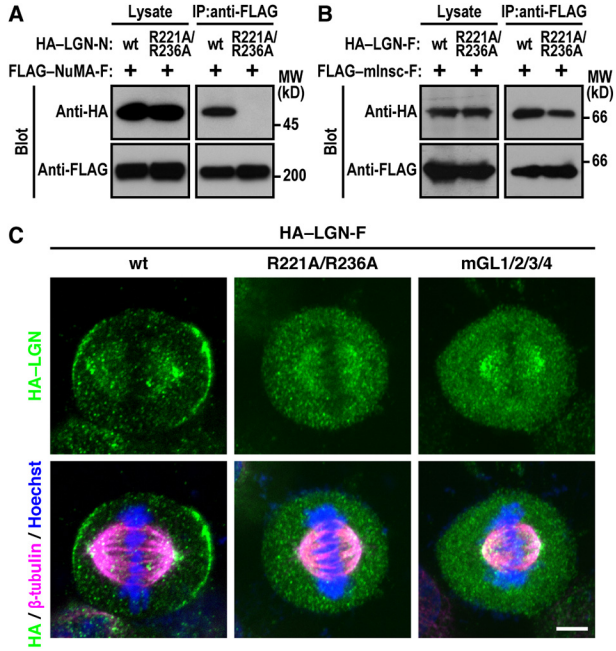

Figure 6. LGN is recruited to the cell cortex during metaphase in a manner dependent on its simultaneous binding to NuMA and Gα_i. *A*, FLAG–NuMA-F was co-expressed with HA–LGN-N (wt) or HA–LGN-N (R221A/R236A) in HEK293 cells. *B*, FLAG–mInsc-F was co-expressed with HA–LGN-F (wt) or HA–LGN-F (R221A/R236A) in HEK293 cells. Proteins in the cell lysate were immunoprecipitated (*IP*) with the anti-FLAG antibody, followed by immunoblot analysis with the indicated antibodies (*Blot*). Positions for marker proteins are indicated in kilodaltons. *MW*, molecular weight. *C*, HeLa cells expressing HA–LGN (wt), HA–LGN (R221A/R236A), or HA–LGN-mGL1/2/3/4 at metaphase were fixed and stained using the anti-HA (*green*) and anti–β-tubulin (*magenta*) antibodies and Hoechst (*blue*). *Scale bar*, 5 μm.

TPR domain with a C-terminal region that contains four GL motifs (GL1–GL4) (8). Although the significant role of GL3 and GL4 in the autoinhibited structure has been well demonstrated (28), states of other GL motifs have remained to be elucidated. As shown in the present binding assay using separate N- and C-terminal fragments (Fig. 1), GL3 and GL4 are essential for interaction with the TPR domain, and the interaction is strongly enhanced by the linker between GL2 and GL3; by contrast, neither GL1 nor GL2 seems to play a major role in the intramolecular interaction. As a result, GL1 is easily accessible to its target protein Gα_i even in a closed structure of LGN (Figs. 2 and 3). This is well documented by the following findings: a full-length LGN with intact GL1 and the other GL motifs mutated (LGN-F-mGL2/3/4) binds to Gα_i to the same extent as does the WT protein, whereas inactivation of GL1 impairs the interaction of full-length LGN with Gα_i (Fig. 2), and LGN-F-mGL2/3/4 harboring intact GL1 but not proteins with inactivated GL1 is recruited to the plasma membrane in Gα_i-overexpressing cells (Fig. 3). In contrast to GL1, the other three GL motifs are normally in a state inaccessible to Gα_i (Figs. 2 and 3). This is compatible with the observation that Gα_i-interacting residues of GL3 and GL4 are masked in an autoinhibited, closed structure of truncated LGN (28). On the other hand, the inaccessibility of GL2 to Gα_i may be explicable by the involvement of its C-terminally flanking region in the intramolecular interaction, although GL2 by itself does not make a major contribution to the closed structure of LGN.

The present model for a closed form of LGN is somewhat different from that proposed by Pan *et al.* (28), in which GL1/2 (the pair of GL1 and GL2) and GL3/4 (the pair of GL3 and GL4) both interact with the N-terminal TPR domain, albeit GL3/4 has a higher affinity than that of GL1/2. The reason for the discrepancy is presently unknown, but it may be possible that less attention has been paid to the role of the linker region between GL2 and GL3. On the other hand, the closed structure of LGN with easily accessible GL1 is similar to that proposed for Pins, a *Drosophila* homolog of mammalian LGN (29), which lacks a motif corresponding to GL2 in LGN and thus has only three GL motifs (30). In Pins, the second and third GL motifs (corresponding to GL3 and GL4 in LGN, respectively) play a crucial role in the autoinhibited intramolecular interaction (29). Of note, the linker region between GL2 and GL3, playing a crucial role in human LGN (Fig. 1, *B* and *C*), is evolutionarily conserved in mammalian LGN and *Drosophila* Pins (Fig. 1*A*), although the role for this region of Pins has not been tested. Because the linker region, as well as GL3 and GL4, is also conserved in AGS3 (Fig. 1*A*), a mammalian protein that has the same domain architecture as that of LGN and participates in directed migration of neutrophils (33), its function may be similarly regulated via the intramolecular interaction.

Although LGN, in a closed state, interacts via GL1 with Gα_i but is normally inaccessible to NuMA (Fig. 4*C*), Gα_i and NuMA cooperatively induce a conformational change of LGN to enhance binding to both proteins (Fig. 4, *A* and *C*). Consistent with this, cortical localization of LGN requires its simultaneous interaction with Gα_i and NuMA during metaphase in nonpolarized symmetrically dividing HeLa cells (Fig. 6*C*). In contrast to NuMA, mInsc efficiently binds to LGN even in the absence of Gα_i (Fig. 4, *B* and *D*) and induces a conformational change to enhance binding to Gα_i (Figs. 4, *A* and *B*, and 5*B*). With its high affinity for LGN, mInsc replaces NuMA at the cortical crescents in metaphase HeLa cells and perturbs planar orientation of mitotic spindles (Fig. 7). This finding appears to agree with previous observations that depletion of LGN impairs both cortical localization of NuMA and planar spindle orientation during metaphase in HeLa cells (10–13). Intriguingly, planar spindle orientation is perturbed but not strongly randomized even by the severe decrease in cortical localization of the dynein-binding protein NuMA (Fig. 7*C*), which may implicate the existence of an additional pathway to maintain planar spindle orientation during metaphase. In this context, it should be noted that, even in the absence of astral microtubules, metaphase spindles in HeLa and MDCK cells are not randomly positioned along the *x*–*z* plane, but the orientation remains biased toward a shallow spindle tilt along the *x*–*z* dimension (34).

In polarized mammalian cells such as epidermal and neuronal progenitor cells, mInsc localizes to the apical membrane, which leads to apical recruitment of LGN and converts from planar into oblique/vertical orientation of mitotic spindles for asymmetric cell division (14, 16–19). In these cases, it is assumed that NuMA is recruited to the apical domain via binding to LGN, which is transported by the LGN–mInsc interaction. The assumption may not be simply accepted, because mInsc and NuMA interact with LGN in a mutually exclusive manner. In asymmetric cell division of neuronal progenitor

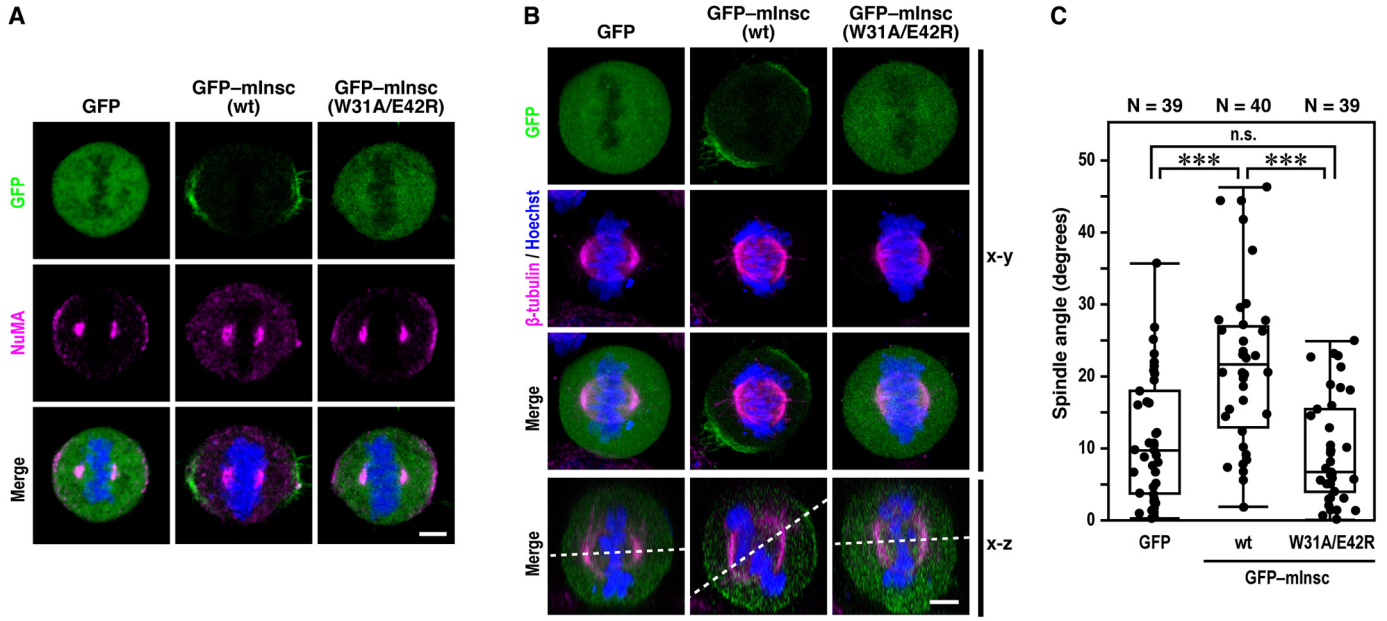

Figure 7. Exogenous mInsc inhibits cortical localization of NuMA and correct spindle orientation during metaphase. *A* and *B*, representative confocal images of HeLa cells expressing GFP alone, GFP–mInsc (wt), or GFP–mInsc (W31A/E42R), visualized by GFP (*green*) and with the anti-NuMA (*A*) or anti-β-tubulin (*B*) antibody (*magenta*), and Hoechst (*blue*). Cross-sectional *Z*-stack analysis (*x-z*) is also shown in *B*. *White dashed lines* indicate spindle axes. *C*, scatter diagrams and box-and-whisker plots of metaphase spindle angles in cells expressing GFP alone, GFP–mInsc (wt), or GFP–mInsc (W31A/E42R). ***, $p < 0.001$ (Steel–Dwass test). *Scale bars*, 5 μm; *n.s.*, not significant.

cells in the mammalian neocortex, mInsc does not drive strictly vertical orientations (17); planar spindle orientation may be an active process of orienting the spindle, whereas oblique and vertical orientations may reflect a more passive result of inhibiting this orienting machinery (35). This mechanism may function in mInsc-expressing HeLa cells, where mInsc perturbs the orienting machinery by decreasing cortical NuMA, leading to oblique spindle orientation (Fig. 7).

It has been reported that, even in LGN-deficient cells, NuMA localizes to cortical crescents during anaphase via interacting with other proteins such as the cytoskeletal protein Band 4.1 and its related proteins or with membrane phosphoinositides (36–38). Since these proteins and lipids interact with NuMA at regions other than the LGN-binding site, it seems likely that NuMA is normally recruited to the lateral cortex even in cells that ectopically express mInsc (wt). Unexpectedly, however, expression of mInsc (wt) strongly inhibits cortical localization of NuMA without impairing its localization to the two spindle poles during anaphase in HeLa cells (Fig. 8), suggesting that LGN plays a major role in cortical localization of NuMA in anaphase, as well as metaphase. Furthermore, mInsc (wt) but not mInsc (W31A/E42R) appears to retard cell cycle progression from metaphase to anaphase (Fig. 8). The role of NuMA in this process can be highlighted here by using mInsc as a tool to specifically inhibit cortical recruitment of NuMA; on the other hand, because global depletion of NuMA results in early-stage mitotic defects in mammalian cells (39–41), it seems to be difficult to dissect the specific contribution of cortical NuMA at the metaphase–anaphase transition.

It is presently unknown about the mechanism whereby blockade of the LGN–NuMA interaction leads to the delay of anaphase onset. It has been reported that LGN is required for normal cell cycle progression (42–44) and that NuMA contributes to efficient chromosome separation but not to anaphase initiation (45). The delay of anaphase onset in mInsc-expressing HeLa cells (Fig. 8) does not seem to result from mitotic spindle misorientation, because checkpoint systems that inhibit anaphase onset until the spindle is properly positioned are considered to be absent (4, 36). On the other hand, a possible link of correct spindle orientation to anaphase onset has been demonstrated (46–49). For instance, O'Connell and Wang (46) have reported, using unperturbed NRK (normal rat kidney) cells, that anaphase onset is significantly delayed in cells containing an incorrectly aligned spindle, although anaphase can start before the spindle reaches its final position. In mitotic HeLa cells, depletion of LIM kinase, which phosphorylates and thereby inactivates the actin-depolymerizing protein cofilin, perturbs cortical accumulation of LGN and mitotic spindle orientation, leading to the delay of anaphase onset (48). Further studies should be addressed to know the precise role of LGN and NuMA in regulation of anaphase onset.

Experimental procedures

Plasmid construction

The cDNAs encoding human $G\alpha_{i2}$ (amino acids 1–355), $G\alpha_{i2}$ with an internal Glu-Glu tag ($G\alpha_{i2}$–EE), LGN (amino acids 1–677), and mInsc (amino acids 1–532) were prepared as previously described (15, 33, 50, 51), and the cDNA for human MuMA of 2101 amino acids (52) was generous gift from Prof. Duane A. Compton (Dartmouth Medical School, Hanover, NH). The cDNA fragments for various regions of these proteins were amplified by PCR using specific primers and their respective full-length cDNAs as templates. Mutations leading to the indicated amino acid substitutions were generated by PCR-mediated site-directed mutagenesis. The cDNAs were ligated into

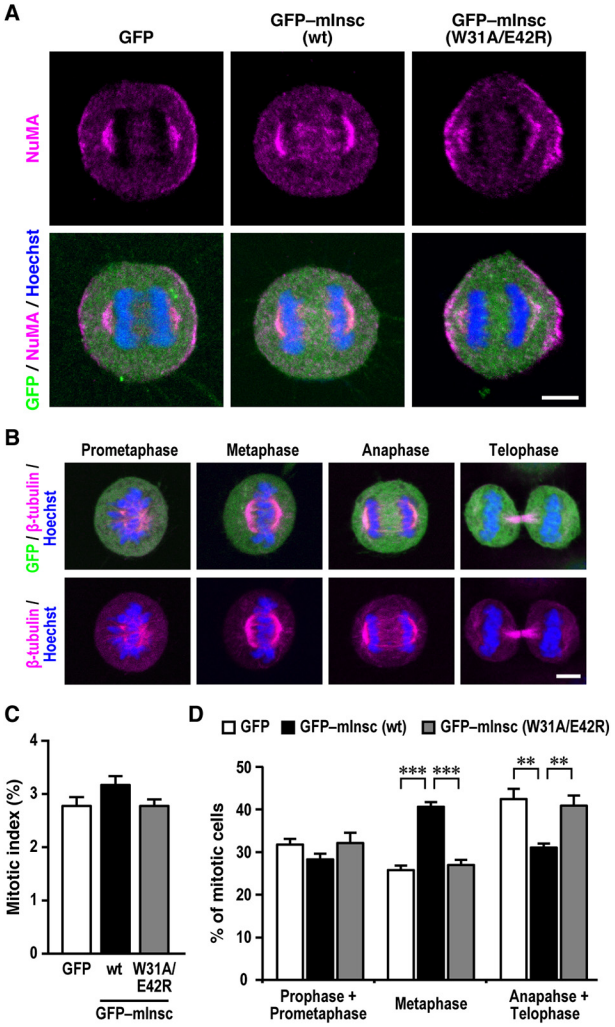

Figure 8. Exogenous mInsc inhibits cortical localization of NuMA in anaphase and blocks mitotic progression from metaphase to anaphase. *A*, representative confocal images of HeLa cells expressing GFP alone, GFP–mInsc (wt), or GFP–mInsc (W31A/E42R), visualized by GFP (*green*) and with the anti-NuMA antibody (*magenta*) and Hoechst (*blue*). *B*, representative confocal images of GFP-expressing HeLa cells at different mitotic stages. The cells were fixed and stained with the anti-β-tubulin antibody (*magenta*) and Hoechst (*blue*). *C*, the mitotic index of HeLa cells expressing GFP alone, GFP–mInsc (wt), or GFP–mInsc (W31A/E42R). The values are means ± S.D. from three independent experiments ($n > 1000$ cells/experiment). *D*, quantification of HeLa cells expressing GFP alone, GFP–mInsc (wt), or GFP–mInsc (W31A/E42R) at different mitotic stages. The values are means ± S.D. from three independent experiments ($n > 350$ cells/experiment). **, $p < 0.01$; and ***, $p < 0.001$ (Tukey–Kramer multiple comparison test). *Scale bars*, 5 μm.

the following expression vectors: pGEX-6P (GE Healthcare) for expression as glutathione *S*-transferase (GST)-fused proteins in *Escherichia coli*; pRSFDuet-1 (Novagen) for bacterial expression of LGN proteins with an N-terminal His_6 (His)-tag followed by a rhinovirus 3C protease cleavage site or with an N-terminal MBP-tag, a subsequent 3C protease cleavage site, and a C-terminal His-tag (20, 23); pEGFP-C1 (Clontech) for expression of N-terminally GFP-tagged mInsc in mammalian cells; pEF-BOS for expression of FLAG-, Myc-, or HA-tagged proteins in mammalian cells (53); and pcDNA3 (Thermo Fisher Scientific) for expression of EE-tagged $G\alpha_{i2}$ in mammalian cells (50, 51). All of the constructs were sequenced for confirmation of their identities.

Antibodies and reagents

Anti-FLAG (M2; catalog no. F3165) and anti-β-tubulin (TUB 2.1; catalog no. T4026) mouse monoclonal antibodies were purchased from Sigma–Aldrich; anti-Glu-Glu (EE) mouse mAb (catalog no. MMS-115P) from Covance; anti-Myc mouse monoclonal (9E10; catalog no. 11 67 203 001) and anti-HA (3F10; catalog no. 11 867 431 001) rat monoclonal antibodies from Roche Applied Science; anti-NuMA mouse mAb (Ab-2; catalog no. NA09L) from Calbiochem; and control mouse IgG1 from DakoCytomation (catalog no. X0931).

Cell culture and transfection with cDNA

The human embryonic kidney HEK293T cells and HeLa cells were cultured in Dulbecco's modified Eagle's medium (DMEM) with 10% fetal calf serum (FCS), and MDCK II cells were cultured in Eagle's minimal essential medium with 10% FCS. The cells were transfected with the following plasmid vectors: pEF-BOS for expression as FLAG-, Myc-, and HA-tagged protein; pcDNA3 for expression as EE-tagged protein; and pEGFP-C1 for expression as GFP-tagged protein. Transfection was performed using X-tremeGENE HP DNA transfection reagent (Roche Applied Science) for HEK293T and HeLa cells or using Nucleofector (Lonza) for MDCK II cells.

Generation of MDCK cells stably expressing $G\alpha_{i2}$

MDCKII cells that stably expressed EE-tagged $G\alpha_{i2}$ (wt) were generated, according to the method as previously described (53). Briefly, MDCKII cells were transfected with the $G\alpha_{i2}$–EE cDNA ligated to pcDNA3 (Thermo Fisher Scientific) using Ronza Nucleofector and subsequently selected in the presence of G418 (600 μg/ml).

An in vitro pulldown binding assay

The indicated C-terminal fragments of LGN were expressed in *E. coli* strain BL21 (DE3) as a protein carrying both N-terminal MBP and C-terminal His-tag, and purified with amylose resin (New England BioLabs) and cOmplete His-tag purificatin resin (Roche Applied Science). Full-length LGN proteins were expressed as a fusion with both N-terminal MBP and C-terminal His tag and purified using cOmplete His tag purification resin, followed by cleavage of the MBP moiety with 3C PreScission protease (GE Healthcare). LGN-N (13–414) and $G\alpha_{i2}$ (G204A) were expressed as His- or GST-fusion protein and purified as previously described (23, 33). GST–LGN-N were purified with glutathione–Sepharose 4B (GE Healthcare), and MBP–NuMA and MBP–mInsc were purified with amylose resin. These proteins were further purified by gel-filtration chromatography using HiLoad 26/600 Superdex 200 column (GE Healthcare).

For an *in vitro* binding assay, purified proteins were incubated for 15 min at 4 °C in binding buffer (150 mM NaCl, 2 mM DTT, 2 mM EDTA, 0.02% Triton X-100, and 20 mM HEPES, pH 7.4) and pulled down with amylose resin, COSMOGEL® His-Accept (Nacalai Tesque), or glutathione-Sepharose 4B. The precipitated proteins were then subjected to SDS-PAGE, followed by staining with Coomassie Brilliant Blue (CBB).

Immunoprecipitation and immunoblot analysis

HEK 293T cells were transfected with pEF-BOS for expression as FLAG-, Myc-, or HA-tagged protein and with pcDNA3 for expression as EE-tagged protein. Transfected cells were cultured for 24 or 36 h in DMEM with 10% FCS and lysed by sonication at 4 °C in lysis buffer (150 mM NaCl, 0.1% Triton X-100, 1 mM DTT, 1 mM EDTA, 10% glycerol, and 50 mM HEPES, pH 7.5) supplemented with Protease inhibitor mixture (Sigma–Aldrich). Proteins in the cell lysate were immunoprecipitated using the anti-FLAG antibody (M2) and protein G–Sepharose (GE Healthcare), as previously described (33, 41, 50, 53). The precipitants were analyzed by immunoblot with the anti-FLAG (M2), anti-Myc (9E10), or anti-EE mAb. The blots were developed using ImmunoStar (FUJIFILM Wako Pure Chemical) for visualization of antibodies.

Immunofluorescent microscopy

Immunofluorescence microscopy was performed as previously described (33, 41, 51, 53). For staining of β-tubulin and HA- and EE-tagged proteins, MDCK and HeLa cells grown on glass coverslips were fixed for 10 min in 3.7% formaldehyde at room temperature and permeabilized for 20 min with 0.5% Triton X-100 in PBS (137 mM NaCl, 2.7 mM KCl, 8.1 mM Na_2HPO_4, and 1.5 mM KH_2PO_4, pH 7.4) containing 3% BSA. For staining of NuMA, HeLa cells were fixed for 15 min in 3.7% formaldehyde at 37 °C and then for 5 min in 100% methanol at −20 °C, followed by permeabilization for 20 min in PBS containing 0.5% Triton X-100 and 3% BSA. The samples were incubated overnight at 4 °C with the indicated primary antibodies in PBS containing 3% BSA and subsequently incubated for 45 min at room temperature with secondary antibodies in PBS containing 3% BSA. Immunofluorescence analysis was performed using the following secondary antibody: Alexa Fluor 488-labeled goat anti-rat antibodies (Thermo Fisher Scientific) or Alexa Fluor 488-labeled goat anti-mouse IgG antibodies (Thermo Fisher Scientific). Nuclei were stained with Hoechst 33342 (Thermo Fisher Scientific). Confocal images were captured at room temperature on the confocal microscope LSM700 (Carl Zeiss) and analyzed using ZEN (Carl Zeiss) and Fiji/ImageJ (version 2.0; National Institutes of Health). The microscopes were equipped with a Plan-Apochromat 63×/1.4 NA oil-immersion objective lens or a C-Apochromat 40×/1.2 NA W Corr water-immersion objective lens.

Measurement of the spindle angle and statistical analysis

HeLa cells were cultured in DMEM with 10% FCS, and 2.0×10^4 cells were seeded onto glass-bottomed imaging dishes (Matsunami; catalog no. D11130H) for 6 h to adhere. The cells were further cultured in DMEM without FCS for 18 h and subsequently transfected with pEGFP-C1 encoding the GFP–mInsc. Transfected cells were fixed for 15 min with 3.7% formaldehyde and subsequently permeabilized and blocked for 30 min with 0.5% Triton X-100 in PBS containing 3% BSA. Fixed cells were incubated with the indicated antibodies and subsequently with Alexa-labeled secondary antibodies and Hoechst 33342. Stained metaphase cells were analyzed with a LSM 700 confocal microscope using a 63× objective lens. Mitotic spindle axis angles were measured in images of *x-z* optimal sections passing through the spindle poles at least three independent experiments using the angle tool of Fiji/ImageJ software. The data showed a non-Gaussian distribution and were statistically analyzed using Steel–Dwass test. The criterion for statistical significance was set up at $p < 0.05$. The figure panels were arranged using ImageJ, Photoshop, and Illustrator (Adobe).

Quantification of mitotic phases and statistical analysis

HeLa cells transfected with pEGFP-C1 encoding GFP–mInsc were grown on glass coverslips for 24 h, fixed for 15 min in 3.7% formaldehyde at 37 °C, and permeabilized for 30 min with 0.5% Triton X-100 in PBS containing 3% BSA. The cells were incubated overnight at 4 °C with anti-β-tubulin antibodies and subsequently with Alexa-labeled secondary antibodies and Hoechst 33342. The mitotic index was calculated as the percentage of mitotic GFP-positive cells with condensed chromatin/total GFP-positive cells, and mitotic phases of GFP-positive cells were counted by the visual inspection of chromatin, β-tubulin, and cell shape (54, 55). The cells were grouped into different phases of mitosis according to the morphology of DNA and the mitotic spindles. The data were statistically analyzed by Tukey–Kramer test, and the criterion for statistical significance was set at $p < 0.05$.

Author contributions—H. T., J. H., S. K., K. M., and H. S. conceptualization; H. T., J. H., S. K., K. C., S. Y., and H. S. data curation; H. T., J. H., S. K., K. M., K. C., S. Y., and H. S. formal analysis; H. T., J. H., S. K., K. M., and H. S. supervision; H. T., J. H., S. K., K. M., K. C., S. Y., and H. S. methodology; H. T., J. H., and H. S. writing-original draft; H. T., J. H., S. K., K. M., and H. S. writing-review and editing.

Acknowledgments—We thank Prof. Duane A. Compton (Dartmouth Medical School) for generously providing the cDNA for human NuMA; Namiko Kubo (Kyushu University) for technical assistance; and Hiromi Takeyama (Kyushu University) for secretarial assistance. We also appreciate technical support from the Research Support Center, Research Center for Human Disease Modeling, Kyushu University Graduate School of Medical Sciences.

References

1. Knoblich, J. A. (2010) Asymmetric cell division: recent developments and their implications for tumour biology. *Nat. Rev. Mol. Cell Biol.* **11,** 849–860 CrossRef Medline
2. Morin, X., and Bellaïche, Y. (2011) Mitotic spindle orientation in asymmetric and symmetric cell divisions during animal development. *Dev. Cell* **21,** 102–119 CrossRef Medline
3. Williams, S. E., and Fuchs, E. (2013) Oriented divisions, fate decisions. *Curr. Opin. Cell Biol.* **25,** 749–758 CrossRef Medline
4. Kiyomitsu, T. (2015) Mechanisms of daughter cell-size control during cell division. *Trends Cell Biol.* **25,** 286–295 CrossRef Medline
5. di Pietro, F., Echard, A., and Morin, X. (2016) Regulation of mitotic spindle orientation: an integrated view. *EMBO Rep.* **17,** 1106–1130 CrossRef Medline
6. Tuncay, H., and Ebnet, K. (2016) Cell adhesion molecule control of planar spindle orientation. *Cell Mol. Life Sci.* **73,** 1195–1207 CrossRef Medline
7. Bergstralh, D. T., Dawney, N. S., and St Johnston, D. (2017) Spindle orientation: a question of complex positioning. *Development* **144,** 1137–1145 CrossRef Medline
8. Du, Q., and Macara, I. G. (2004) Mammalian Pins is a conformational switch that links NuMA to heterotrimeric G proteins. *Cell* **119,** 503–516 CrossRef Medline
9. Woodard, G. E., Huang, N. N., Cho, H., Miki, T., Tall, G. G., and Kehrl, J. H. (2010) Ric-8A and Giα recruit LGN, NuMA, and dynein to the cell

cortex to help orient the mitotic spindle. *Mol. Cell Biol.* **30,** 3519–3530 CrossRef Medline
10. Zheng, Z., Zhu, H., Wan, Q., Liu, J., Xiao, Z., Siderovski, D. P., and Du, Q. (2010) LGN regulates mitotic spindle orientation during epithelial morphogenesis. *J. Cell Biol.* **189,** 275–288 CrossRef Medline
11. Matsumura, S., Hamasaki, M., Yamamoto, T., Ebisuya, M., Sato, M., Nishida, E., and Toyoshima, F. (2012) ABL1 regulates spindle orientation in adherent cells and mammalian skin. *Nat. Commun.* **3,** 626 CrossRef Medline
12. Kotak, S., Busso, C., and Gönczy, P. (2012) Cortical dynein is critical for proper spindle positioning in human cells. *J. Cell Biol.* **199,** 97–110 CrossRef Medline
13. Kiyomitsu, T., and Cheeseman, I. M. (2012) Chromosome- and spindle-pole-derived signals generate an intrinsic code for spindle position and orientation. *Nat. Cell Biol.* **14,** 311–317 CrossRef Medline
14. Lechler, T., and Fuchs, E. (2005) Asymmetric cell divisions promote stratification and differentiation of mammalian skin. *Nature* **437,** 275–280 CrossRef Medline
15. Izaki, T., Kamakura, S., Kohjima, M., and Sumimoto, H. (2006) Two forms of human Inscuteable-related protein that links Par3 to the Pins homologues LGN and AGS3. *Biochem. Biophys. Res. Commun.* **341,** 1001–1006 CrossRef Medline
16. Poulson, N. D., and Lechler, T. (2010) Robust control of mitotic spindle orientation in the developing epidermis. *J. Cell Biol.* **191,** 915–922 CrossRef Medline
17. Postiglione, M. P., Jüschke, C., Xie, Y., Haas, G. A., Charalambous, C., and Knoblich, J. A. (2011) Mouse Inscuteable induces apical-basal spindle orientation to facilitate intermediate progenitor generation in the developing neocortex. *Neuron* **72,** 269–284 CrossRef Medline
18. Williams, S. E., Beronja, S., Pasolli, H. A., and Fuchs, E. (2011) Asymmetric cell divisions promote Notch-dependent epidermal differentiation. *Nature* **470,** 353–358 CrossRef Medline
19. Williams, S. E., Ratliff, L. A., Postiglione, M. P., Knoblich, J. A., and Fuchs, E. (2014) Par3–mInsc and $G\alpha_{i3}$ cooperate to promote oriented epidermal cell divisions through LGN. *Nat. Cell Biol.* **16,** 758–769 CrossRef Medline
20. Yuzawa, S., Kamakura, S., Iwakiri, Y., Hayase, J., and Sumimoto, H. (2011) Structural basis for interaction between the conserved cell polarity proteins Inscuteable and Leu-Gly-Asn repeat–enriched protein (LGN). *Proc. Natl. Acad. Sci. U.S.A.* **108,** 19210–19215 CrossRef Medline
21. Zhu, J., Wen, W., Zheng, Z., Shang, Y., Wei, Z., Xiao, Z., Pan, Z., Du, Q., Wang, W., and Zhang, M. (2011) LGN/mInsc and LGN/NuMA complex structures suggest distinct functions in asymmetric cell division for the Par3/mInsc/LGN and $G\alpha_i$/LGN/NuMA pathways. *Mol. Cell* **43,** 418–431 CrossRef Medline
22. Culurgioni, S., Alfieri, A., Pendolino, V., Laddomada, F., and Mapelli, M. (2011) Inscuteable and NuMA proteins bind competitively to Leu-Gly-Asn repeat–enriched protein (LGN) during asymmetric cell divisions. *Proc. Natl. Acad. Sci. U.S.A.* **108,** 20998–21003 CrossRef Medline
23. Takayanagi, H., Yuzawa, S., and Sumimoto, H. (2015) Structural basis for the recognition of the scaffold protein Frmpd4/Preso1 by the TPR domain of the adaptor protein LGN. *Acta Crystallogr. F Struct. Biol. Commun.* **71,** 175–183 CrossRef Medline
24. Culurgioni, S., Mari, S., Bonetti, P., Gallini, S., Bonetto, G., Brennich, M., Round, A., Nicassio, F., and Mapelli, M. (2018) Insc:LGN tetramers promote asymmetric divisions of mammary stem cells. *Nat. Commun.* **9,** 1025 CrossRef Medline
25. Pirovano, L., Culurgioni, S., Carminati, M., Alfieri, A., Monzani, S., Cecatiello, V., Gaddoni, C., Rizzelli, F., Foadi, J., Pasqualato, S., and Mapelli, M. (2019) Hexameric NuMA:LGN structures promote multivalent interactions required for planar epithelial divisions. *Nat. Commun.* **10,** 2208 CrossRef Medline
26. McCudden, C. R., Willard, F. S., Kimple, R. J., Johnston, C. A., Hains, M. D., Jones, M. B., and Siderovski, D. P. (2005) $G\alpha$ selectivity and inhibitor function of the multiple GoLoco motif protein GPSM2/LGN. *Biochim. Biophys. Acta* **1745,** 254–264 CrossRef Medline
27. Jia, M., Li, J., Zhu, J., Wen, W., Zhang, M., and Wang, W. (2012) Crystal structures of the scaffolding protein LGN reveal the general mechanism by which GoLoco binding motifs inhibit the release of GDP from $G\alpha_i$. *J. Biol. Chem.* **287,** 36766–36776 CrossRef Medline
28. Pan, Z., Zhu, J., Shang, Y., Wei, Z., Jia, M., Xia, C., Wen, W., Wang, W., and Zhang, M. (2013) An autoinhibited conformation of LGN reveals a distinct interaction mode between GoLoco motifs and TPR motifs. *Structure* **21,** 1007–1017 CrossRef Medline
29. Nipper, R. W., Siller, K. H., Smith, N. R., Doe, C. Q., and Prehoda, K. E. (2007) $G\alpha_i$ generates multiple Pins activation states to link cortical polarity and spindle orientation in *Drosophila* neuroblasts. *Proc. Natl. Acad. Sci. U.S.A.* **104,** 14306–14311 CrossRef Medline
30. Willard, F. S., Kimple, R. J., and Siderovski, D. P. (2004) Return of the GDI: the GoLoco motif in cell division. *Annu. Rev. Biochem.* **73,** 925–951 CrossRef Medline
31. Takesono, A., Cismowski, M. J., Ribas, C., Bernard, M., Chung, P., Hazard, S., 3rd, Duzic, E., and Lanier, S. M. (1999) Receptor-independent activators of heterotrimeric G-protein signaling pathways. *J. Biol. Chem.* **274,** 33202–33205 CrossRef Medline
32. May, K. M., and Hardwick, K. G. (2006) The spindle check point. *J. Cell Sci.* **119,** 4139–4142 CrossRef Medline
33. Kamakura, S., Nomura, M., Hayase, J., Iwakiri, Y., Nishikimi, A., Takayanagi, R., Fukui, Y., and Sumimoto, H. (2013) The cell polarity protein mInsc regulates neutrophil chemotaxis via a noncanonical G protein signaling pathway. *Dev. Cell* **26,** 292–302 CrossRef Medline
34. Lázaro-Diéguez, F., Ispolatov, I., and Müsch, A. (2015) Cell shape impacts on the positioning of the mitotic spindle with respect to the substratum. *Mol. Biol. Cell* **26,** 1286–1295 CrossRef Medline
35. Lancaster, M. A., and Knoblich, J. A. (2012) Spindle orientation in mammalian cerebral cortical development. *Curr. Opin. Neurobiol.* **22,** 737–746 CrossRef Medline
36. Kiyomitsu, T., and Cheeseman, I. M. (2013) Cortical dynein and asymmetric membrane elongation coordinately position the spindle in anaphase. *Cell* **154,** 391–402 CrossRef Medline
37. Seldin, L., Poulson, N. D., Foote, H. P., and Lechler, T. (2013) NuMA localization, stability, and function in spindle orientation involve 4.1 and Cdk1 interactions. *Mol. Biol. Cell* **24,** 3651–3662 CrossRef Medline
38. Kotak, S., Busso, C., and Gönczy, P. (2014) NuMA interacts with phosphoinositides and links the mitotic spindle with the plasma membrane. *EMBO J.* **33,** 1815–1830 CrossRef Medline
39. Compton, D. A., and Cleveland, D. W. (1993) NuMA is required for the proper completion of mitosis. *J. Cell Biol.* **120,** 947–957 CrossRef Medline
40. Radulescu, A. E., and Cleveland, D. W. (2010) NuMA after 30 years: the matrix revisited. *Trends Cell Biol.* **20,** 214–222 CrossRef Medline
41. Iwakiri, Y., Kamakura, S., Hayase, J., and Sumimoto, H. (2013) Interaction of NuMA protein with the kinesin Eg5: its possible role in bipolar spindle assembly and chromosome alignment. *Biochem. J.* **451,** 195–204 CrossRef Medline
42. Du, Q., Stukenberg, P. T., and Macara, I. G. (2001) A mammalian partner of Inscuteable binds NuMA and regulates mitotic spindle organization. *Nat. Cell Biol.* **3,** 1069–1075 CrossRef Medline
43. Kaushik, R., Yu, F., Chia, W., Yang, X., and Bahri, S. (2003) Subcellular localization of LGN during mitosis: evidence for its cortical localization in mitotic cell culture systems and its requirement for normal cell cycle progression. *Mol. Biol. Cell* **14,** 3144–3155 CrossRef Medline
44. Yasumi, M., Sakisaka, T., Hoshino, T., Kimura, T., Sakamoto, Y., Yamanaka, T., Ohno, S., and Takai, Y. (2005) Direct binding of Lgl2 to LGN during mitosis and its requirement for normal cell division. *J. Biol. Chem.* **280,** 6761–6765 CrossRef Medline
45. Zheng, Z., Wan, Q., Meixiong, G., and Du, Q. (2014) Cell cycle–regulated membrane binding of NuMA contributes to efficient anaphase chromosome separation. *Mol. Biol. Cell* **25,** 606–619 CrossRef Medline
46. O'Connell, C. B., and Wang, Y. L. (2000) Mammalian spindle orientation and position respond to changes in cell shape in a dynein-dependent fashion. *Mol. Biol. Cell* **11,** 1765–1774 CrossRef Medline
47. Haydar, T. F., Ang, E., Jr., and Rakic, P. (2003) Mitotic spindle rotation and mode of cell division in the developing telencephalon. *Proc. Natl. Acad. Sci. U.S.A.* **100,** 2890–2895 CrossRef Medline
48. Kaji, N., Muramoto, A., and Mizuno, K. (2008) LIM kinase-mediated Cofilin phosphorylation during mitosis is required for precise spindle positioning. *J. Biol. Chem.* **283,** 4983–4992 CrossRef Medline

49. Larson, M. E., and Bement, W. M. (2017) Automated mitotic spindle tracking suggests a link between spindle dynamics, spindle orientation, and anaphase onset in epithelial cells. *Mol. Biol. Cell* **28,** 746–759 CrossRef Medline
50. Chishiki, K., Kamakura, S., Yuzawa, S., Hayase, J., and Sumimoto, H. (2013) Ubiquitination of the heterotrimeric G protein α subunits $G\alpha_{i2}$ and $G\alpha_q$ is prevented by the guanine nucleotide exchange factor Ric-8A. *Biochem. Biophys. Res. Commun.* **435,** 414–419 CrossRef Medline
51. Chishiki, K., Kamakura, S., Hayase, J., and Sumimoto, H. (2017) Ric-8A, an activator protein of $G\alpha_i$, controls mammalian epithelial cell polarity for tight junction assembly and cystogenesis. *Genes Cells* **22,** 293–309 CrossRef Medline
52. Compton, D. A., Szilak, I., and Cleveland, D. W. (1992) Primary structure of NuMA, an intranuclear protein that defines a novel pathway for segregation of proteins at mitosis. *J. Cell Biol.* **116,** 1395–1408 CrossRef Medline
53. Hayase, J., Kamakura, S., Iwakiri, Y., Yamaguchi, Y., Izaki, T., Ito, T., and Sumimoto, H. (2013) The WD40 protein Morg1 facilitates Par6–aPKC binding to Crb3 for apical identity in epithelial cells. *J. Cell Biol.* **200,** 635–650 CrossRef Medline
54. Eves, E. M., Shapiro, P., Naik, K., Klein, U. R., Trakul, N., and Rosner, M. R. (2006) Raf kinase inhibitory protein regulates aurora B kinase and the spindle checkpoint. *Mol. Cell* **23,** 561–574 CrossRef Medline
55. Chapard, C., Meraldi, P., Gleich, T., Bachmann, D., Hohl, D., and Huber, M. (2014) TRAIP is a regulator of the spindle assembly checkpoint. *J. Cell Sci.* **127,** 5149–5156 CrossRef Medline